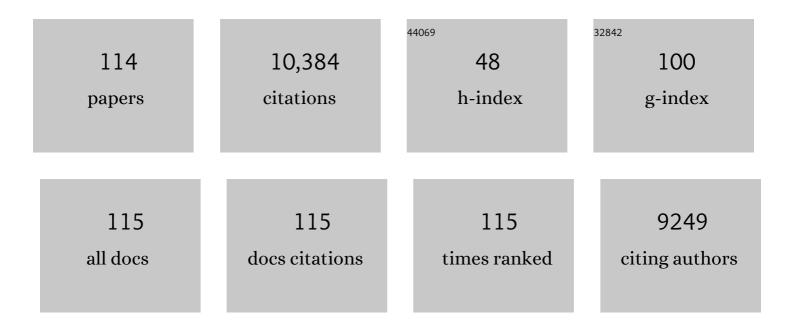
## David L Buckley

List of Publications by Year in descending order

Source: https://exaly.com/author-pdf/794323/publications.pdf Version: 2024-02-01



#	Article	IF	CITATIONS
1	Estimating kinetic parameters from dynamic contrast-enhanced t1-weighted MRI of a diffusable tracer: Standardized quantities and symbols. Journal of Magnetic Resonance Imaging, 1999, 10, 223-232.	3.4	2,856
2	Imaging biomarker roadmap for cancer studies. Nature Reviews Clinical Oncology, 2017, 14, 169-186.	27.6	792
3	Experimentally-derived functional form for a population-averaged high-temporal-resolution arterial input function for dynamic contrast-enhanced MRI. Magnetic Resonance in Medicine, 2006, 56, 993-1000.	3.0	574
4	Classic models for dynamic contrastâ€enhanced MRI. NMR in Biomedicine, 2013, 26, 1004-1027.	2.8	324
5	On the scope and interpretation of the Tofts models for DCEâ€MRI. Magnetic Resonance in Medicine, 2011, 66, 735-745.	3.0	295
6	Tracer kinetic modelling in MRI: estimating perfusion and capillary permeability. Physics in Medicine and Biology, 2012, 57, R1-R33.	3.0	289
7	Uncertainty in the analysis of tracer kinetics using dynamic contrast-enhancedT1-weighted MRI. Magnetic Resonance in Medicine, 2002, 47, 601-606.	3.0	257
8	Prostate Cancer: Evaluation of Vascular Characteristics with Dynamic Contrast-enhanced T1-weighted MR Imaging—Initial Experience. Radiology, 2004, 233, 709-715.	7.3	204
9	Microvessel density in invasive breast cancer assessed by dynamic gd-dtpa enhanced MRI. Journal of Magnetic Resonance Imaging, 1997, 7, 461-464.	3.4	173
10	Blockade of Platelet-Derived Growth Factor Receptor-Beta by CDP860, a Humanized, PEGylated di-Fab', Leads to Fluid Accumulation and Is Associated With Increased Tumor Vascularized Volume. Journal of Clinical Oncology, 2005, 23, 973-981.	1.6	167
11	Prediction of radiotherapy outcome using dynamic contrast enhanced MRI of carcinoma of the cervix. International Journal of Radiation Oncology Biology Physics, 2002, 54, 759-767.	0.8	165
12	Quantitative imaging biomarkers in the clinical development of targeted therapeutics: current and future perspectives. Lancet Oncology, The, 2008, 9, 766-776.	10.7	150
13	Tumour volume determination from MR images by morphological segmentation. Physics in Medicine and Biology, 1996, 41, 2437-2446.	3.0	144
14	Imaging vascular function for early stage clinical trials using dynamic contrast-enhanced magnetic resonance imaging. European Radiology, 2012, 22, 1451-1464.	4.5	138
15	Visualization of neural tissue water compartments using biexponential diffusion tensor MRI. Magnetic Resonance in Medicine, 2001, 45, 580-587.	3.0	118
16	Measurement of single kidney function using dynamic contrast-enhanced MRI: Comparison of two models in human subjects. Journal of Magnetic Resonance Imaging, 2006, 24, 1117-1123.	3.4	118
17	ls volume transfer coefficient (K(trans)) related to histologic grade in human gliomas?. American Journal of Neuroradiology, 2005, 26, 2455-65.	2.4	109
18	Preliminary Study of Oxygen-Enhanced Longitudinal Relaxation in MRI: A Potential Novel Biomarker of Oxygenation Changes in Solid Tumors. International Journal of Radiation Oncology Biology Physics, 2009, 75, 1209-1215.	0.8	107

#	Article	IF	CITATIONS
19	Differentiation of prostatic carcinoma and benign prostatic hyperplasia: Correlation between dynamic Gd-DTPA-enhanced MR imaging and histopathology. Journal of Magnetic Resonance Imaging, 1999, 9, 311-316.	3.4	106
20	Magnetic resonance imaging screening in women at genetic risk of breast cancer: imaging and analysis protocol for the UK multicentre study. Magnetic Resonance Imaging, 2000, 18, 765-776.	1.8	104
21	Precision in measurements of perfusion and microvascular permeability withT1-weighted dynamic contrast-enhanced MRI. Magnetic Resonance in Medicine, 2006, 56, 986-992.	3.0	93
22	MR microscopy of multicomponent diffusion in single neurons. Magnetic Resonance in Medicine, 2001, 46, 1107-1112.	3.0	92
23	A comparison of tracer kinetic models for <i>T</i> <sub>1</sub> -weighted dynamic contrast-enhanced MRI: Application in carcinoma of the cervix. Magnetic Resonance in Medicine, 2010, 63, 691-700.	3.0	92
24	The effect of ouabain on water diffusion in the rat hippocampal slice measured by high resolution NMR imaging. Magnetic Resonance in Medicine, 1999, 41, 137-142.	3.0	90
25	Comparative study of methods for determining vascular permeability and blood volume in human gliomas. Journal of Magnetic Resonance Imaging, 2004, 20, 748-757.	3.4	90
26	Computer Threeâ€Dimensional Anatomical Reconstruction of the Human Sinus Node and a Novel Paranodal Area. Anatomical Record, 2011, 294, 970-979.	1.4	89
27	Quantitative analysis of multi-slice Gd-DTPA enhanced dynamic MR images using an automated simplex minimization procedure. Magnetic Resonance in Medicine, 1994, 32, 646-651.	3.0	88
28	Dynamic MR imaging of invasive breast cancer: correlation with tumour grade and other histological factors British Journal of Radiology, 1997, 70, 446-451.	2.2	82
29	Dynamic MR imaging of the breast combined with analysis of contrast agent kinetics in the differentiation of primary breast tumours. Clinical Radiology, 1997, 52, 516-526.	1.1	78
30	Comparison of normal tissue <i>R</i> <sub><i>1</i></sub> and <i>R</i> modulation by oxygen and carbogen. Magnetic Resonance in Medicine, 2009, 61, 75-83.	3.0	77
31	Observer variability in the interpretation of contrast enhanced MRI of the breast. British Journal of Radiology, 1996, 69, 1009-1016.	2.2	76
32	Organâ€specific effects of oxygen and carbogen gas inhalation on tissue longitudinal relaxation times. Magnetic Resonance in Medicine, 2007, 58, 490-496.	3.0	75
33	Cellularâ€interstitial water exchange and its effect on the determination of contrast agent concentration in vivo: Dynamic contrastâ€enhanced MRI of human internal obturator muscle. Magnetic Resonance in Medicine, 2008, 60, 1011-1019.	3.0	71
34	Dynamic MRI of Invasive Breast Cancer: Assessment of Three Region-of-Interest Analysis Methods. Journal of Computer Assisted Tomography, 1997, 21, 431-438.	0.9	70
35	BOLD imaging: a potential predictive biomarker of renal functional outcome following revascularization in atheromatous renovascular disease. Nephrology Dialysis Transplantation, 2012, 27, 1013-1019.	0.7	68
36	Prediction of axillary lymph node status in invasive breast cancer with dynamic contrast-enhanced MR imaging Radiology, 1997, 203, 317-321.	7.3	67

#	Article	IF	CITATIONS
37	Estrogens Decrease Reperfusion-Associated Cortical Ischemic Damage. Stroke, 2001, 32, 987-992.	2.0	66
38	Dynamic Contrast-Enhanced Magnetic Resonance Imaging of the Breast Combined with Pharmacokinetic Analysis of Gadolinium-DTPA Uptake in the Diagnosis of Local Recurrence of Early Stage Breast Carcinoma. Investigative Radiology, 1995, 30, 650-662.	6.2	65
39	Two-component diffusion tensor MRI of isolated perfused hearts. Magnetic Resonance in Medicine, 2001, 45, 1039-1045.	3.0	63
40	Perfusion Estimated With Rapid Dynamic Contrast-Enhanced Magnetic Resonance Imaging Correlates Inversely With Vascular Endothelial Growth Factor Expression and Pimonidazole Staining in Head-and-Neck Cancer: A Pilot Study. International Journal of Radiation Oncology Biology Physics, 2011, 81, 1176-1183.	0.8	63
41	The effect of blood inflow and <i>B</i> <sub>1</sub> â€field inhomogeneity on measurement of the arterial input function in axial 3D spoiled gradient echo dynamic contrastâ€enhanced MRI. Magnetic Resonance in Medicine, 2011, 65, 108-119.	3.0	61
42	Dynamic gradient-echo and fat-suppressed spin-echo contrast-enhanced MRI of the breast. Clinical Radiology, 1995, 50, 440-454.	1.1	60
43	A comparison of Ktransmeasurements obtained with conventional and first pass pharmacokinetic models in human gliomas. Journal of Magnetic Resonance Imaging, 2004, 19, 527-536.	3.4	60
44	Modeling of contrast agent kinetics in the lung using <i>T</i> <sub>1</sub> â€weighted dynamic contrastâ€enhanced MRI. Magnetic Resonance in Medicine, 2009, 61, 1507-1514.	3.0	58
45	Gadoliniumâ€enhanced magnetic resonance imaging for renovascular disease and nephrogenic systemic fibrosis: Critical review of the literature and UK experience. Journal of Magnetic Resonance Imaging, 2009, 29, 887-894.	3.4	54
46	MR-derived renal morphology and renal function in patients with atherosclerotic renovascular disease. Kidney International, 2006, 69, 715-722.	5.2	53
47	Imaging vascular physiology to monitor cancer treatment. Critical Reviews in Oncology/Hematology, 2006, 58, 95-113.	4.4	53
48	Enhancing fraction measured using dynamic contrast-enhanced MRI predicts disease-free survival in patients with carcinoma of the cervix. British Journal of Cancer, 2010, 102, 23-26.	6.4	52
49	Consensus-based technical recommendations for clinical translation of renal T1 and T2 mapping MRI. Magnetic Resonance Materials in Physics, Biology, and Medicine, 2020, 33, 163-176.	2.0	52
50	Functional, Anatomical, and Molecular Investigation of the Cardiac Conduction System and Arrhythmogenic Atrioventricular Ring Tissue in the Rat Heart. Journal of the American Heart Association, 2013, 2, e000246.	3.7	50
51	Benign prostatic hyperplasia: Evaluation of T <sub>1</sub> , T <sub>2</sub> , and microvascular characteristics with T <sub>1</sub> â€weighted dynamic contrastâ€enhanced MRI. Journal of Magnetic Resonance Imaging, 2009, 29, 641-648.	3.4	48
52	Assessment of Bladder Motion for Clinical Radiotherapy Practice Using Cine–Magnetic Resonance Imaging. International Journal of Radiation Oncology Biology Physics, 2009, 75, 664-671.	0.8	47
53	A Systematic Review of the Clinical Implementation of Pelvic Magnetic Resonance Imaging–Only Planning for External Beam Radiation Therapy. International Journal of Radiation Oncology Biology Physics, 2019, 105, 479-492.	0.8	47
54	Effects of renal volume and single-kidney glomerular filtration rate on renal functional outcome in atherosclerotic renal artery stenosis. Nephrology Dialysis Transplantation, 2010, 25, 1133-1140.	0.7	42

#	Article	IF	CITATIONS
55	Tracer Kinetic Modelling for T1-Weighted DCE-MRI. , 2005, , 81-92.		41
56	Myocardial blood flow at rest and stress measured with dynamic contrastâ€enhanced MRI: Comparison of a distributed parameter model with a fermi function model. Magnetic Resonance in Medicine, 2013, 70, 1591-1597.	3.0	41
57	Multi-parametric MRI-guided focal tumor boost using HDR prostate brachytherapy: A feasibility study. Brachytherapy, 2014, 13, 137-145.	0.5	41
58	Measuring Contrast Agent Concentration in T1-Weighted Dynamic Contrast-Enhanced MRI. , 2005, , 69-79.		40
59	Prediction and assessment of responses to renal artery revascularization with dynamic contrast-enhanced magnetic resonance imaging: a pilot study. American Journal of Physiology - Renal Physiology, 2013, 305, F672-F678.	2.7	40
60	In Vivo Prostate Magnetic Resonance Imaging and Magnetic Resonance Spectroscopy at 3 Tesla Using a Transceive Pelvic Phased Array Coil. Investigative Radiology, 2003, 38, 443-451.	6.2	36
61	Tracer kinetic analysis of dynamic contrastâ€enhanced MRI and CT bladder cancer data: A preliminary comparison to assess the magnitude of water exchange effects. Magnetic Resonance in Medicine, 2010, 64, 595-603.	3.0	35
62	What levels of precision are achievable for quantification of perfusion and capillary permeability surface area product using ASL?. Magnetic Resonance in Medicine, 2007, 58, 281-289.	3.0	34
63	Multicentre, deep learning, synthetic-CT generation for ano-rectal MR-only radiotherapy treatment planning. Radiotherapy and Oncology, 2021, 156, 23-28.	0.6	33
64	Transcytolemmal water exchange and its affect on the determination of contrast agent concentration in vivo. Magnetic Resonance in Medicine, 2002, 47, 420-421.	3.0	32
65	Comparison of errors associated with single- and multi-bolus injection protocols in low-temporal-resolution dynamic contrast-enhanced tracer kinetic analysis. Magnetic Resonance in Medicine, 2006, 56, 611-619.	3.0	32
66	MR microscopy of perfused brain slices. Magnetic Resonance in Medicine, 1997, 38, 1012-1015.	3.0	31
67	Incidental significant arrhythmia in scleroderma associates with cardiac magnetic resonance measure of fibrosis and hs-TnI and NT-proBNP. Rheumatology, 2019, 58, 1221-1226.	1.9	31
68	Heterogeneity Analysis of Gd-DTPA Uptake: Improvement in Breast Lesion Differentiation. Journal of Computer Assisted Tomography, 1999, 23, 615-621.	0.9	29
69	Nuclear magnetic resonance imaging measurements of water diffusion in the perfused hippocampal slice during N-methyl-d-aspartate-induced excitotoxicity. Neuroscience, 1999, 93, 487-490.	2.3	26
70	Late tissue effects following radiotherapy and neoadjuvant hormone therapy of the prostate measured with quantitative magnetic resonance imaging. Radiotherapy and Oncology, 2008, 88, 127-134.	0.6	26
71	MR imaging measurement of compartmental water diffusion in perfused heart slices. American Journal of Physiology - Heart and Circulatory Physiology, 2001, 281, H1280-H1285.	3.2	25
72	Fingers: three-dimensional MR imaging and angiography with a local gradient coil Radiology, 1994, 190, 895-899.	7.3	22

#	Article	IF	CITATIONS
73	Kidney volume to GFR ratio predicts functional improvement after revascularization in atheromatous renal artery stenosis. PLoS ONE, 2017, 12, e0177178.	2.5	22
74	Comparison of dynamic contrastâ€enhanced MRI and dynamic contrastâ€enhanced CT biomarkers in bladder cancer. Magnetic Resonance in Medicine, 2011, 66, 219-226.	3.0	20
75	A functional form for a representative individual arterial input function measured from a population using high temporal resolution DCE MRI. Magnetic Resonance in Medicine, 2019, 81, 1955-1963.	3.0	20
76	Estimating breast tumor blood flow during neoadjuvant chemotherapy using interleaved high temporal and high spatial resolution MRI. Magnetic Resonance in Medicine, 2018, 79, 317-326.	3.0	17
77	NMR microscopy—beginnings and new directions. Magnetic Resonance Materials in Physics, Biology, and Medicine, 1999, 9, 112-116.	2.0	15
78	Sensitivity of quantitative myocardial dynamic contrastâ€enhanced MRI to saturation pulse efficiency, noise and t 1 measurement error: Comparison of nonlinearity correction methods. Magnetic Resonance in Medicine, 2016, 75, 1290-1300.	3.0	14
79	In vivo dynamics and distribution of intracerebroventricularly administered gadodiamide, visualized by magnetic resonance imaging. Neuroscience, 1999, 90, 1115-1122.	2.3	13
80	Gadofosvesetâ€based biomarker of tissue albumin concentration: Technical validation in vitro and feasibility in vivo. Magnetic Resonance in Medicine, 2015, 73, 244-253.	3.0	13
81	Rapid Skill Capture in a First-Person Shooter. IEEE Transactions on Games, 2017, 9, 63-75.	1.4	13
82	Shutterâ€speed dynamic contrastâ€enhanced MRI: Is it fit for purpose?. Magnetic Resonance in Medicine, 2019, 81, 976-988.	3.0	13
83	Effect of Temporal Resolution on the Diagnostic Efficacy of Contrast-Enhanced MRI in the Conservatively Treated Breast. Journal of Computer Assisted Tomography, 1998, 22, 47-51.	0.9	13
84	Predicting skill from gameplay input to a first-person shooter. , 2013, , .		11
85	Estimating kinetic parameters from dynamic contrast-enhanced t1-weighted MRI of a diffusable tracer: Standardized quantities and symbols. , 0, .		11
86	Overcoming the low relaxivity of gadofosveset at high field with spin locking. Magnetic Resonance in Medicine, 2012, 68, 1234-1238.	3.0	10
87	MRI measurement of cell volume fraction in the perfused rat hippocampal slice. Magnetic Resonance in Medicine, 1999, 42, 603-607.	3.0	9
88	Evaluation of Monoexponential, Stretchedâ€Exponential and Intravoxel Incoherent Motion <scp>MRI</scp> Diffusion Models in Early Response Monitoring to Neoadjuvant Chemotherapy in Patients With Breast Cancer—A Preliminary Study. Journal of Magnetic Resonance Imaging, 2022, 56, 1079-1088.	3.4	8
89	NMR microscopy — beginnings and new directions. Magnetic Resonance Materials in Physics, Biology, and Medicine, 1999, 9, 112-116.	2.0	7
90	Analytical validation of single-kidney glomerular filtration rate and split renal function as measured with magnetic resonance renography. Magnetic Resonance Imaging, 2019, 59, 53-60.	1.8	7

#	Article	IF	CITATIONS
91	Bias and Precision in Magnetic Resonance Imagingâ€Based Estimates of Renal Blood Flow: Assessment by Triangulation. Journal of Magnetic Resonance Imaging, 2021, , .	3.4	7
92	The effects of cryoablation on renal cell carcinoma perfusion and glomerular filtration rate measured using dynamic contrast-enhanced MRI: A feasibility study. Clinical Radiology, 2013, 68, 887-894.	1.1	6
93	Renal Cell Carcinoma Perfusion before and after Radiofrequency Ablation Measured with Dynamic Contrast Enhanced MRI: A Pilot Study. Diagnostics, 2018, 8, 3.	2.6	6
94	Improved peripheral MR angiography with temperature regulation in healthy patients Radiology, 1996, 198, 899-902.	7.3	5
95	Localization of MR-detected breast cancer using a prototype stereotactic guidance MR system. Breast, 1997, 6, 65-68.	2.2	5
96	Title is missing!. Investigative Radiology, 2003, 38, 443-451.	6.2	5
97	The benefit of MRâ€only radiotherapy treatment planning for anal and rectal cancers: A planning study. Journal of Applied Clinical Medical Physics, 2021, 22, 41-53.	1.9	5
98	Are Measurements from Two Commercial Software Packages Interchangeable? Possibly, If Like Is Compared with Like. Radiology, 2008, 246, 642-643.	7.3	4
99	Feasibility of MRI based extracellular volume fraction and partition coefficient measurements in thigh muscle. British Journal of Radiology, 2020, 93, 20190931.	2.2	4
100	Dynamic contrast enhanced MR. Clinical Radiology, 1996, 51, 78-79.	1.1	3
101	Breast tumour volume and blood flow measured by MRI after one cycle of epirubicin and cyclophosphamide-based neoadjuvant chemotherapy as predictors of pathological response. British Journal of Radiology, 2021, 94, 20201396.	2.2	3
102	Feasibility Study on Using Dynamic Contrast Enhanced MRI to Assess the Effect of Tyrosine Kinase Inhibitor Therapy within the STAR Trial of Metastatic Renal Cell Cancer. Diagnostics, 2021, 11, 1302.	2.6	3
103	Optimization of the DCE-CT protocol using active imaging. , 2010, , .		2
104	Implementation of Image Reconstruction for GE SIGNA PET/MR PET Data in the STIR Library. , 2018, , .		2
105	Motion correction of free-breathing magnetic resonance renography using model-driven registration. Magnetic Resonance Materials in Physics, Biology, and Medicine, 2021, 34, 805-822.	2.0	2
106	Patient position verification in magnetic-resonance imaging only radiotherapy of anal and rectal cancers. Physics and Imaging in Radiation Oncology, 2021, 19, 72-77.	2.9	2
107	Quantitative analysis of GD-DTPA enhanced dynamic MR images by simplex minimization. Magnetic Resonance Materials in Physics, Biology, and Medicine, 1994, 2, 413-416.	2.0	1
108	3D MRI and angiography of human extremities using a local gradient coil. Magnetic Resonance Materials in Physics, Biology, and Medicine, 1994, 2, 461-465.	2.0	1

#	Article	IF	CITATIONS
109	Imaging perfusion and blood–brain barrier permeability using T1-weighted dynamic contrast-enhanced MR imaging. , 0, , 113-128.		1
110	Pre-clinical assessment of anti-vascular drugs using quantitative dynamic contrast-enhanced MRI. International Journal of Medical Engineering and Informatics, 2012, 4, 362.	0.3	1
111	Diffusion-Weighted Magnetic Resonance Imaging of the Breast: an Accurate Method for Measuring Early Response to Neoadjuvant Chemotherapy?. Current Breast Cancer Reports, 2019, 11, 74-82.	1.0	1
112	Exploratory Analysis of Serial 18F-fluciclovine PET-CT and Multiparametric MRI during Chemoradiation for Glioblastoma. Cancers, 2022, 14, 3485.	3.7	1
113	Myocardial microvascular function at rest and stress measured with dynamic contrast-enhanced MRI. Journal of Cardiovascular Magnetic Resonance, 2012, 14, .	3.3	0
114	Establishment of the National Cancer Research Institute Clinical and Translational Radiotherapy Research Working Group (CTRad) Biomarker Support Network. Clinical Oncology, 2014, 26, 356.	1.4	0